International Journal of Engineering Research and Development
e-ISSN: 2278-067X, p-ISSN: 2278-800X, www.ijerd.com
Volume 10, Issue 4 (April 2014), PP.20-28

Microstructural Characterization and Pits Morphology Analysis on Austenitic Stainless Steel Aisi 304

(1,2)Rosinei B. Ribeiro, (1,2,3)José W. J. Silva, (4)Bianca S. M. Domingos, (5)Jorge L. Rosa and (2,3)Nilo A. S. Sampaio
(1)Faculdades Integradas Teresa D'Ávila – FATEA – Rede Salesianas – Lorena – SP - Brazil
(2) Universidade do Estado do Rio de Janeiro – UERJ – Resende – RJ – Brazil
(3)Associação Educacional Dom Bosco – AEDB – Resende – RJ – Brazil
(4)Universidade Federal de Itajubá – UNIFEI – Itajubá – MG – Brazil
(5)Escola de Engenharia de Lorena – USP – Lorena – SP – Brazil

Abstract:- This paper aims to study the evolution establishing distribution and classification of pits in austenitic stainless steels AISI 304 obtained in state as received and heat-treated under different exposure times via Salt Spray. The work methodology started from the following steps: metallography preparation, corrosion tests via salt spray in different conditions, microstructural analysis, analysis of pits profiles, digital processing and images analysis for purposes of characterizing distribution, morphology and size of pits. In results obtained in digital processing and images analysis of profiles, the data were statistically analyzed using the median as evaluation parameter in the alloy as received and treated. The alloy, as received, exhibited the following morphology: hemispherical pits > transition region A > transition region B > irregular > conical. The pits amount in alloy treated in each exposure time is of the same order: transition region B > Hemispheric > transition region A > conical > irregular.

Keywords:- Pitting Corrosion, Austenitic Stainless Steel 304, Salt Spray, Metallography, Microstructure.

I. INTRODUCTION

Some materials of wide application in engineering, such as stainless steels, Al, Ti and their alloys, for example, are favored with a thin passive oxide layer formation. This layer is formed naturally on the metal surface and it reduces the corrosion rate. Such passive films are often susceptible to localized failure resulting primarily in accelerated dissolution of the material or some of its components [1-3].

Factors related to localized corrosion can initiate or even accelerate structural failures in components in shapes such as holes, pores or cracks leading to fracture. Pitting corrosion can be classified as localized attack resulting in rapid mechanism of metal penetration and removal into small areas. Pits occur by means of several factors that directly influence their formation such as: alloy type, composition, integrity of oxide film layer, other materials presence, manufacturing processes favoring discontinuities production, pores, holes, chemicals and mechanical stress.

Materials and their components are subject to localized corrosion in different environments, which may include carbon steel, stainless steel, titanium, nickel, aluminum and copper. The surfaces of these metals and alloys are passivated when exposed to solutions containing aggressive anions, such as halides (Cl^-, F^-, Br^-).
In these cases, pitting corrosion may be defined as local dissolution leading to formation of cavities, cracks and/or holes [4,5].

The pits morphological classification in materials can vary from its characteristics as shallow shape for cylindrical geometry, pores apparently with hemispherical geometry. Population characteristics and pits morphology aspect in alloys depend on the metallurgical (crystal structure) and chemical (composition) parameters, as well as on environment (bromides, molybdates and chlorides) and their respective concentration conditions. Pits usually cause increased tension and crack nucleation in a use component [6].

Pitting corrosion in aluminum and its alloys is due to four factors: anion adsorption, chemical reaction of absorbed anion with aluminum ion in the aluminum oxide reticle; oxide film penetration by the ion aggressiveness, resulting in dissolution of thin oxide layer and direct attack of the metal exposed by the anion.

The metal susceptibility to pitting corrosion as well as the rate in which occurs localized corrosion depends on the oxide film integrity, however, pits occur in different metals and alloys for many different ways. As an example, Fe-17Cr stainless steel is more susceptible to pitting corrosion in chloride solution than austenitic stainless steel AISI 304, which in relation to the Fe-18Cr-8Ni-3Mo alloy has greater pitting corrosion resistance [7].

In general, titanium and its alloys have resistance superior to the one of the materials presented herein. It is important to avoid an extensive generalization about tendency of an alloy undergoing pitting corrosion.

Thus, occurrence of localized corrosion formation in stainless steel can be observed in solutions containing chloride and bromide ions, hypochlorite or disulfide anions, where pits formation will tend to be eliminated by oxy-anions presence such as NO^-_3 or SO^-_4 [7].

In localized corrosion, it is difficult to predict pits location on metals surface, their distribution and size will depend on structural condition of metal surface beyond the work environment (corrosive environment). The pitting corrosion rate is significantly increased on the metal surface conditions (roughness), nevertheless it is difficult to determine the exact attack extent [8-10].

II. MATERIALS AND METHODS

The material used in this work is austenitic stainless steel AISI 304 provided in plate shape of 10 mm and 6 mm thick in as received state (rolled) and heat-treated at 620 ° C for 24 hours and cooled in air, as in figure 1.

The samples were made in dimensions 30mm x 25mm and superficially prepared (Figure 1). The corrosion tests were carried out via salt spray at the Central Laboratory of TEKNO SA unit Guaratinguetá. The samples were subjected to different exposure times such as 48, 120, 168, 216 and 312 hours.

The solution used in the tests was 5% NaCl at pH 6.7 and process temperature controlled on the order of 35 ° C ± 1.7 ° C, however, exposure zone was fully enclosed cab [11]. The chemical composition of material is shown in Table 1.

Microstructural characterization of material was based on classical materialographic preparation using sandpaper in grain sizes # 220-4000 and polishing with diamond paste of 3μm and 1μm. For microstructural development it was employed a chemical solution with the following reagents: 10 ml HF (48%), 10 mL HNO3 (65%), 15 mL HCl (35%) and two drops of glycerol Pa, for the purposes of studying the grains shape and evaluate type and distribution of precipitates.

It was carried out testing of Vickers microhardness using microdurometer such as Micromet 2004, manufactured by BULHER with load of 100 gF/ mm^2 and indentation time of 15 seconds on a polished surface.
Factors that establish the pits growth in the AISI 304 stainless steel were determined by means of vertical sectioning at low load and rotation speed, then grinding and polishing. To ensure low deformation and region integrity of profile and pits on corroded surface during the mechanical polishing ii was employed epoxy resin after sectioning and a phenolic resin like bakelite for inlay [12]. The morphological and microstructural parameters associated with their changes were characterized after corrosion tests by means of digital image processing and image analysis based on optical microscopy [13].

It was determined the characteristics and morphologies of pits profiles in stainless steel 304, associating statistical data of position and dispersion defining parameters of size, shape description and population, applying the public domain programs UTHSCSA IMAGE TOOL 3.0, IMAGE J and Media Cybernetics Image Pro Plus 4.5/Materials - Analyzer Pro 3.1 carried out in LAIMat-DMT-FEG-UNESP. The shape description is determined by the area-Box (AB) defined as the ratio between the pit area and the area of the smallest box containing the pit, which allows the clear geometry description and quantitative separation of conical, spherical and cylindrical pits among others [14].

III. RESULTS AND DISCUSSION

To simplify the results analysis, the microstructural analysis, microhardness tests, digital processing and image analysis, distribution, morphology and pits size were analyzed individually and subsequently correlated with the steel 304 as received and treated [15,16].

In verification and validation of results obtained in digital processing and images analysis of profiles, data were subjected to statistical analysis, mainly using median of each parameter determined in the alloy [17-19].

Figure 2 shows microstructure in the as received condition characterized by austenite grains typically in steps shape, and the sensitization level in this condition is estimated zero, it is observed presence of deformed regions and the microhardness values increase.

Figure 3, in which the sample was treated at 620ºC for 24 hours, shows the microstructures of original steel character virtually sensitized and micrographs results in grain growth with a high chromium carbides precipitation and in the typically trough shape, due to the high volume fraction and increase in length of grain boundary occurred by presence of chromium carbides precipitates contributing to increased susceptibility to localized corrosion.

The solubilized and sensitized stainless steels display precipitated phases in the most different geometric shapes, due to the heat treatment time started at the grain boundaries.

Table 2, displays material when treated which has lower values in hardness than the state as received, motivated by the high rate of mechanical deformation and its chemical composition.

The micrographs 4 (a), (b) and 5 (a), (b) illustrate, from optical microscopy of profiles, different growth mechanisms of pits associated with microstructural features of alloy in the state received and treated, after being subjected to different exposure times in salt spray.

Pitting corrosion in as-received condition initiates at the grain boundaries and at the interface of mechanically deformed region such as twinned or steps in the grain boundaries. This contributes as a barrier, making difficult the whole mechanism of mass transport (pitting) and decreasing the growth kinetics of localized corrosion in the material, due to the typical microstructure as a step between the boundaries and zero sensitization (precipitation exemption of second phase).

In heat treated condition the pits initiate growth at primary interface of phase induced by precipitation likely $Cr_{23}C_6$ chromium-rich region and the secondary as the whole matrix rich in iron, nickel and chrome especially in grain boundaries in which nucleation is favored and when grains are coalesced and increased by heat treatment (sensitization).

In Table 3 (a), it is visualized the following distribution and classification of pits in stainless steel 304 at each exposure time, it is the same order in pitting amount, that is, transition region A > irregular > conical > hemispherical > transition region B. Cylindrical pits were not observed.

By increasing the exposure time, there is an increase in irregular pits and transition A, but the temporal pits evolution is similar to steel when treated at 620 °C by increasing the hemispherical pits number according to Table 3 (b).

Classification and distribution of pits percentages in stainless steel 304, treated at 620 °C - 24 hours and air cooling.

Table 4 (a) and Figures 8 (a) and (b) show the following order on the size of width median and pits depth associated with pitting morphology: irregular > conical > transition A > hemispherical > transition B, it was observed no existence of cylindrical pits in the system for the stainless steel 304.

Pits geometry is larger in depth than in width and seems to grow rather in width. It was observed that the greater the exposure time in as received condition, the larger the pits width even among the different pits morphologies and the constant depth.

Table 4 (b) displays the following order in median size in width and depth associated with pitting morphology: irregular > conical > transition A > hemispheric > transition B > cylindrical, as in Figures 9 (a) and (b).

Pits appear to be deeper than wide and grow preferentially in depth. It is observed that the higher the exposure time, the greater the pits depth even among the different pits morphologies and constant width.

IV. CONCLUSION

The material after sensitization heat-treatment displayed chromium carbides formation inside and at grain boundaries; particularly stainless steel AISI 304 appeared to be in greater quantity and coarser microstructure contributing to increased pitting corrosion, as data obtained in superficial analysis and in profiles.

On superficial analysis of stainless steel 304 as-received, the following order in pits morphology was displayed: hemispheric > transition region A > transition region B > irregular > conical, and the pits are present in larger amounts in hemispheric and in transition region A. The pits are wider than deep, they preferably grow in width. The cylindrical pits were not observed in the system.

When the material was treated, every exposure time has the same order in pits amount: transition region B > hemispheric > transition region A > conical > irregular, especially the pits are deeper than wide.

Significant changes in morphology distribution and in pits size in stainless steel 304 when treated are correlated to the precipitation character of chromium carbide in its amount and form.

By means of median analysis of size of pits width and depth the following order was proved: irregular > conical > transition region A > Hemisphere > transition region B.

AKNOWLEDGEMENTS

The authors thank all the staff of the EEL-USP, Faculdades Integradas Teresa D`Ávila – FATEA and Centro Universitário de Volta Redonda - Professional Master in Materials - MEMAT-UNIFOA. To TEKNO SA unit Guaratingueta SP for conducting corrosion tests. To PROAP - CAPES and UNESP - Guaratinguetá by supporting the activities carried out during the work.

REFERENCES

[1] Uhlig HH. Corrosion and Corrosion Control. New York: John Willey & Sons; 1967.
[2] Breslin CB, Macdonald DD, Sikora E, Sikola J. Photo-inhibition of pitting on types 304 and 316 stainless steels in chloride containing solution. Electrochimica Acta, 1997; 42: 137-144.
[3] Jayalakshmi M, Muralidharam VS. Empirical and deterministc models of pitting corrosion – an overview, Corrosion reviews, 2011; 14: 375-402.
[4] Ernest P, Laycock NJ, Moayed MH, Newman RC. The mechanism of lacy cover formation in pitting. Corrosion Science, 1997; 39; 1133-1136.
[5] Newman RC, Franz EM. Growth and Repassivation of Single Corrosion Pits in Stainless Steel. 1984; NACE, 40.
[6] Shreir, LL. Corrosion science control. 2nd ed. Newnes-Butterwords: London; 1978.
[7] Szklarska-Smialowska Z. Insight into the pitting corrosion behavior of aluminum alloys. Corrosion Science 1992; 33: 1193-1202.
[8] Frankel GS. Pitting Corrosion of Metals; Review of the Critical Factors. J Electrochemical Society 1998; 145:2186-2198.
[9] Silva JWJ, Bustamante AG, Codaro EN, Nakazato RZ, Hein LRO. Morphological analysis of pits formed on Al 2024-T3 in chloride aqueous solution. Applied Surface Science 2004; 236: 356–365.
[10] Silva JWJ, Codaro EN, Nakazato RZ, Hein LRO. Influence of chromate, molybdate and tungstate on pit formation in chloride medium. Applied Surface Science 2005; 252: 1117–1122.
[11] AMERICAN SOCIETY FOR TESTING AND MATERIALS. ASTM B 117: Standard practice for operation Salt Spray (fog) apparatus, Philadelphia, 1997.
[12] Pereira MC, Silva JWJ, Acciari HA, Codaro EN, Hein LRO. Morphology Characterization and Kinetics Evaluation of Pitting Corrosion of Commercially Pure Aluminium by Digital Image Analysis. Materials Sciences and Applications 2012; 3: 287-293 doi:10.4236/msa.2012.35042.
[13] Ribeiro RB, Silva JWJ, Hein LRO, Pereira MC, Codaro EN, Matias NT. Morphology Characterisation of Pitting Corrosion on Sensitized Austenitic Stainless Steel by Digital Image Analysis. ISRN Corrosion 2013, 2013:1-7. doi:10.1155/2013/905942.
[14] S.S.M. Tavares, V.G. Silva, J.M. Pardal, J.S. Corte, Investigation of stress corrosion cracks in a UNS S32750 superduplex stainless steel, Engineering failure analysis http://dx.doi.org/10.1016/j.engfailanal.2012.12.013
[15] García C, Martín F, Blanco Y, Aparicio ML. Effect of ageing heat treatments on the microstructure and intergranular corrosion of powder metallurgy duplex stainless steels. Corrosion Science 2010, 52, (11): 3725-3737.
[16] Tavares SSM, Moura V, Costa VC, Ferreira MLR, Pardal JM. Microstructural changes and corrosion resistance of AISI 310S steel exposed to 600–800 °C. Materials Characterization 2009, 60: 573-578.
[17] Marano GC, Greco R, Sgobba S. A comparison between different robust optimum design approaches: Application to tuned mass dampers. Probabilistic Engineering Mechanics 2010, 25: 108–118.
[18] Standard Practice for Operating Salt Spray (Fog) Apparatus, ASTM B117-11, 2011, p. 1-10.
[19] Standard Specification for Chromium and Chromium-Nickel Stainless Steels plate, sheet, and strip for pressure vessels and for general applications, ASTM A240/A240M-09a, 2009, pp. 1-13.

Figure Captions

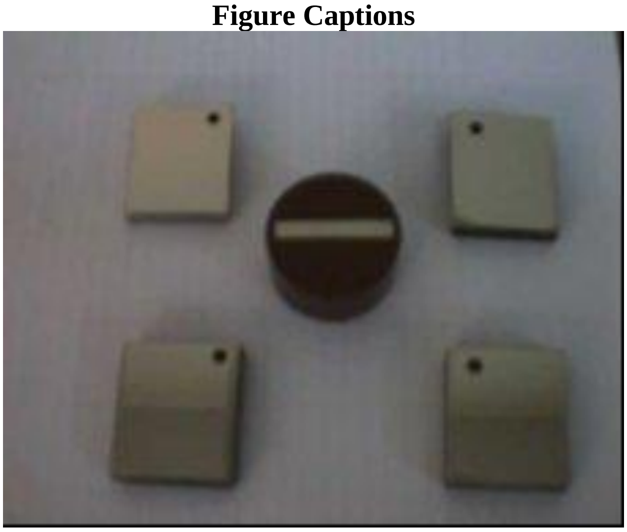

Fig. 1 – Specimens for corrosion testing.

Fig. 2 - Micrograph of AISI 304 stainless steel as received, etched.

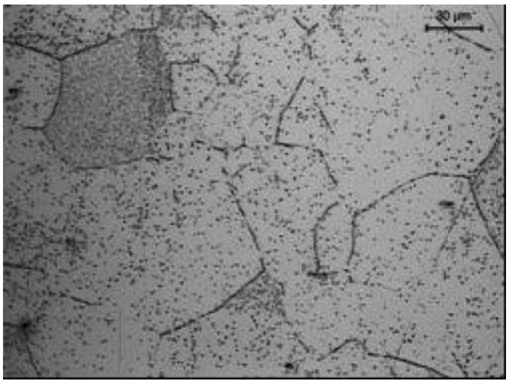

Fig. 3 - Micrograph of 304 stainless steel treated at 620 °C - 24 hours, air cooling, etched.

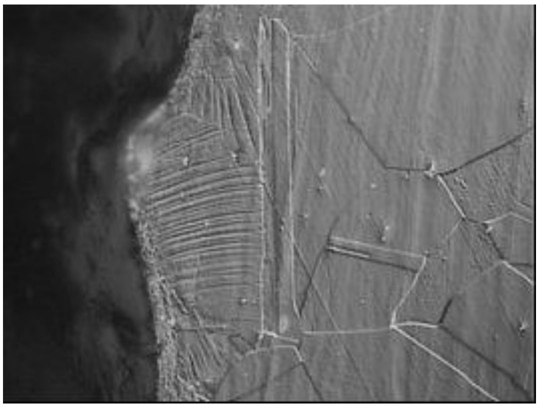

Fig. 4(a) - The occurrence of pitting corrosion on stainless steel 304 in the state as received.

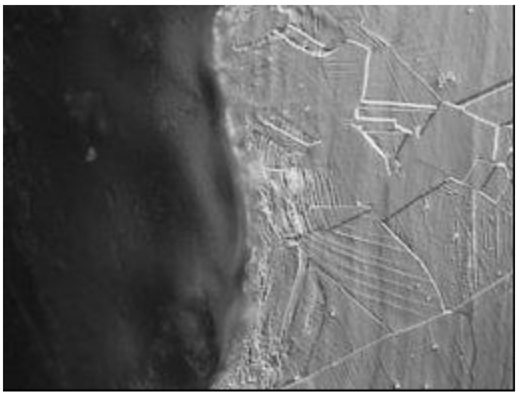

Fig. 4(b) - Occurrence of pitting corrosion on stainless steel 304 in the state as received.

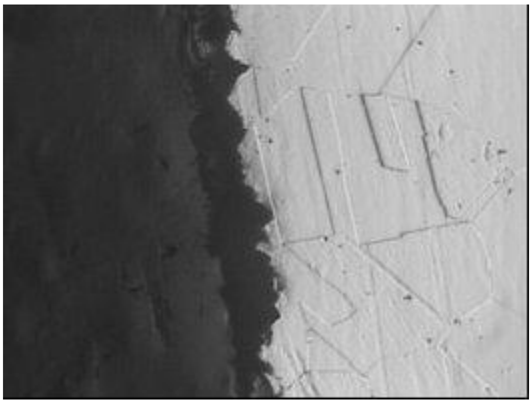

Fig. 5(a) - Occurrence of pitting corrosion in stainless steels 304, treated at 620 °C - 24 hours and air cooling.

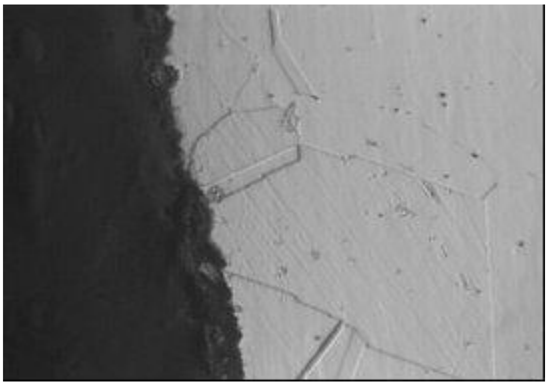

Fig. 5(b) - Occurrence of pitting corrosion in stainless steels 304, treated at 620 °C - 24 hours and air cooling.

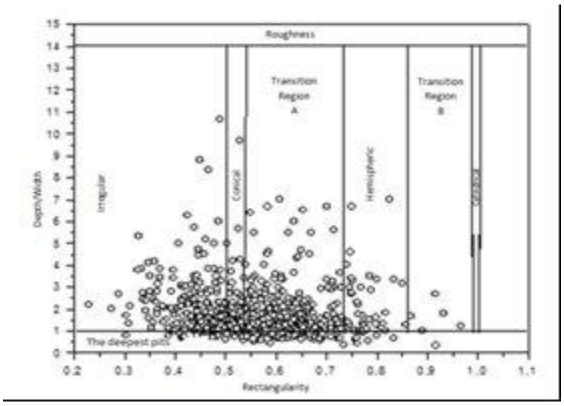

Fig. 6(a) - Classification of pits formed on surface of stainless steel 304 as received, subjected to corrosion tests via salt spray for 48 hours.

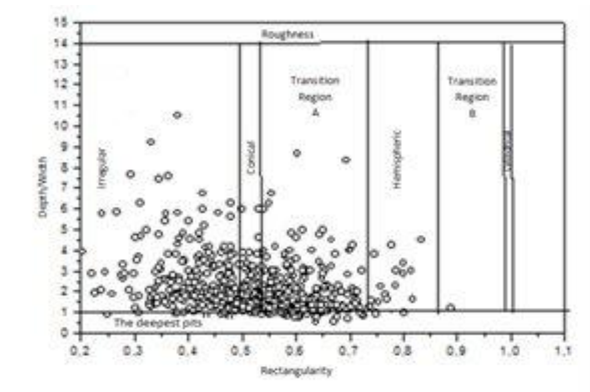

Fig. 6(b) - Classification of pits formed on surface of stainless steel 304 as received, subjected to corrosion tests via salt spray for 312 hours.

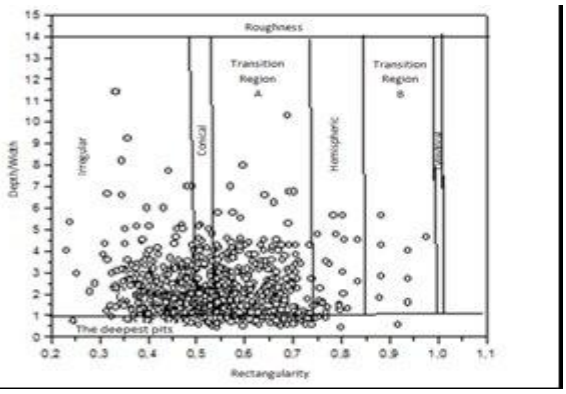

Fig. 7(a) - Classification of pits formed on surface of stainless steel 304 treated at 620 °C for 24 hours and air cooling and subjected to corrosion testing via salt spray for 48 hours.

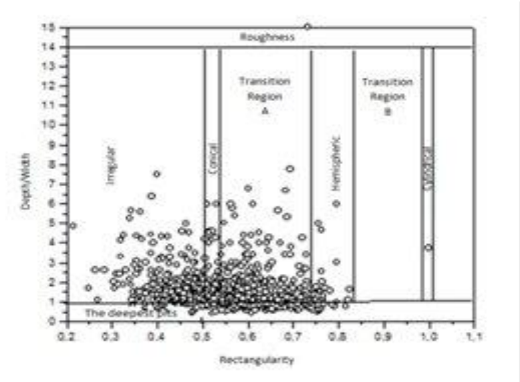

Fig. 7(b) - Classification of pits formed on surface of stainless steel 304 treated at 620 °C for 24 hours and air cooling and subjected to corrosion testing via salt spray for 312 hours.

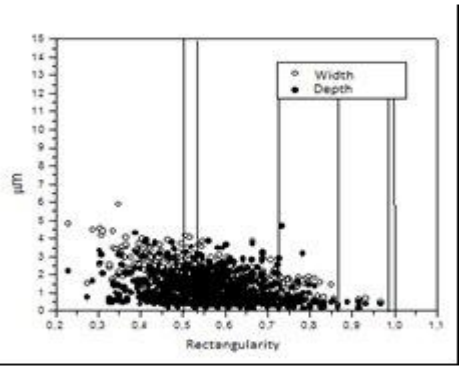

Fig. 8(a) - Size of pits formed on surface of stainless steel 304 in as-received state, after being subjected to corrosion tests via salt spray for 48 h.

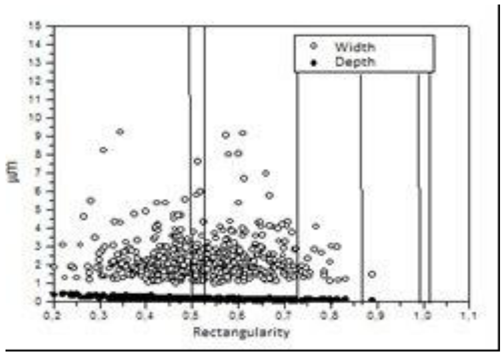

Fig. 8(b) - Size of pits formed on surface of stainless steel 304 in as-received state, after being subjected to corrosion tests via salt spray for 312 h.

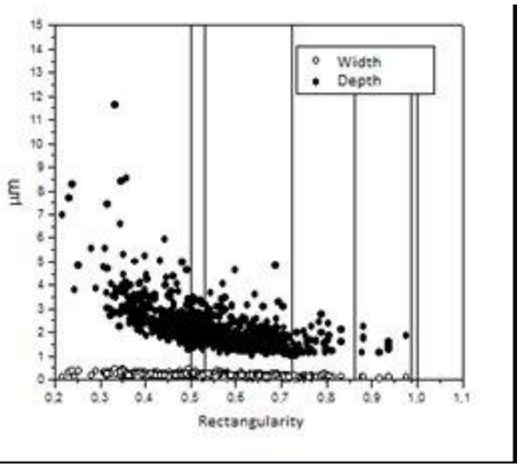

Fig. 9(a) - Size of pits formed on surface of stainless steel 304, treated at 620 °C for 24 hours and air cooling also subjected to corrosion testing via salt fog spray for 48 h.

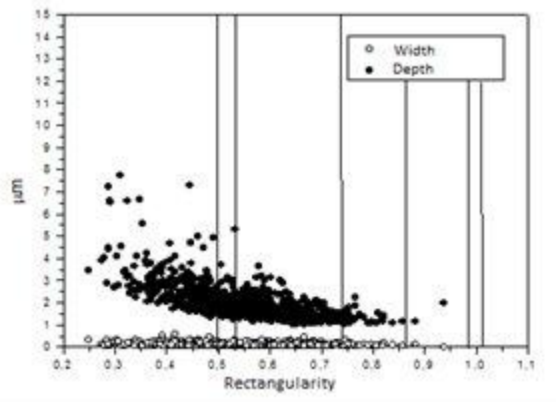

Fig. 9(b) - Size of pits formed on surface of stainless steel 304, treated at 620 °C for 24 hours and air cooling also subjected to corrosion testing via salt spray for 312 h.

TABLES

Table 1

Fe	C	Si	Mn	Cr	Ni	N
Bal.	*0.08*	*1.0*	*2.0*	*18.0*	*10.0*	*0.10*

Chemical composition of AISI 304 Austenitic stainless steel (wt%)

Table 2

Material	Microhardness values - HV	Standard Deviation
Treated at 670 °C - 5 hours, air cooling	173.83	2.33
As received	172.01	1.9

Vickers microhardness values of the austenitic stainless steel AISI 304.

Table 3 (a)

Exposure Time [Hours]	Irregular Pits	Conical Pits	Trans A Pits	Hemispherical Pits	Trans B Pits	Cylindrical Pits
48	24.43	9.39	58.91	8.85	1.6	0
120	31.61	11.87	47.07	8.72	0.71	0
168	30 18	7.04	50.66	11.03	1.06	0
216	45.16	22.57	38.20	5.61	0.44	0
312	43.35	7.85	34.59	3.47	0.15	0

Classification and distribution of pits percentages in stainless steel 304, as received.

Table 3 (b)

Exposure Time [Hours]	Irregular Pits	Conical Pits	Trans A Pits	Hemispherical Pits	Trans B Pits	Cylindrical Pits
48	32.98	9.38	50.97	5.47	1.17	0
120	40.54	9.12	46.45	3.54	0.33	0
168	36.07	9.65	48.01	5.82	0.42	0
216	35.89	10.34	47.02	5.95	0.62	0
312	34.90	9.32	48.04	6.96	0.78	0

Classification and distribution of pits percentages in stainless steeWl 304, treated at 620 °C - 24 Hours and air cooling.

Table 4(a)

Exposure Time [Hours]	Parameters [median] µm	Irregular Pits	Conical Pits	Trans Pits A	Hemispherical Pits	Trans Pits B	Cylindrical Pits
48	width depth	2.54 1.35	1.90 1.26	1.56 1.18	1.08 0.81	0.45 0.35	0 0
120	width depth	0.25 0.11	0.18 0.10	0.16 0.09	0.13 0.07	0.10 0.05	0 0
168	width depth	2.42 1.06	1.56 0.90	1.30 0.71	1.02 0.53	0.80 0.40	0 0
216	width depth	2.36 0.26	2.50 0.16	1.92 0.14	1.77 0.12	1.55 0.12	0 0
312	width depth	3.65 0.22	2.44 0.16	2.16 0.13	2.04 0.11	1.49 0.12	0 0

Width median and pits depth in stainless steel 304, as received.

Table 4(b)

Exposure Time [Hours]	Parameters [median] µm	Irregular Pits	Conical Pits	Trans Pits A	Hemispherical Pits	Trans Pits B	Cylindrical Pits
48	width depth	0.21 2.99	0.17 2.12	0.14 1.80	0.12 1.54	0.11 1.56	0 0
120	width depth	0.22 2.73	0.14 1.90	0.13 1.81	0.12 1.35	0.12 1.42	0 0
168	width depth	0.22 2.78	0.16 2.04	0.14 1.70	0.12 1.36	0.12 2.02	0 0
216	width depth	0.23 3.14	0.19 2.25	0.15 1.80	0.12 1.45	0.10 1.37	0 0
312	width depth	0.13 3.45	0.11 1.90	0.10 1.64	0.10 1.45	0.07 1.18	0 0

Median of width and pits depth in stainless steel 304, treated at 620 °C - 24 hours and air cooling.

Highlights

- Classification of pits in austenitic stainless steels AISI 304.
- Morphology: hemispheric>transition region A>transition region B>irregular>conical.
- Material after sensitization heat-treatment showed chromium carbides inside.
- After sensitization heat-treatment chromium carbides appear at grain boundaries.
- The pits are wider than deep, they preferably grow in width.